Journal of Physiology (1989), **419**, *pp.* 493–508
With 4 text-figures
Printed in Great Britain

ULTRASTRUCTURE OF TRANSPORT PATHWAYS IN STRESSED SYNOVIUM OF THE KNEE IN ANAESTHETIZED RABBITS

BY J. R. LEVICK AND J. N. McDONALD

From the Department of Physiology, St George's Hospital Medical School, London SW17 0RE

(*Received 3 March 1989*)

SUMMARY

1. The hydraulic conductance of the synovial lining of a rabbit knee increases greatly when intra-articular pressure (IAP) is raised above ~ 9 cmH_2O (yield point). To investigate the cause, synovium was fixed *in situ* by perfusion at controlled IAP and prepared for transmission electron microscopy. Micrographs of synovium fixed below yield pressure (atmospheric pressure and 5 cmH_2O IAP, ten joints) and above it (25 cmH_2O IAP, five joints) were analysed by morphometry.

2. The discontinuous cellular lining consisted of fibroblast-like cells (67%) and macrophage-like cells (33%) separated by interstitium-filled gaps. Interstitium formed 26–36% of the surface below yield pressure. Depending on sample site the surface gaps averaged $1{\cdot}9 \pm 0{\cdot}2$ to $2{\cdot}4 \pm 0{\cdot}2$ μm wide below yield pressure (mean ± S.E.M. throughout). Above yield pressure the mean gap width increased by 42–64% ($P < 0{\cdot}05$, analysis of variance).

3. The qualitative and quantitative composition of the lining varied with distance below the surface. In a plane 5 μm deep, the intercellular distances and interstitial area fraction were almost double those at the surface. Classic periodic collagen fibrils (diameter 50 ± 3 nm) abounded at 5 μm depth whereas the surface interstitium was richer in Ruthenium Red-staining microfibrils (diameter $9{\cdot}3 \pm 0{\cdot}7$ nm) associated with 93 nm period fibrous long-spacing bundles.

4. Averaging over all the tissue between the surface and the 5 μm deep plane, the mean interstitial volume fraction was $0{\cdot}61 \pm 0{\cdot}05$ at 5 cmH_2O and $0{\cdot}67 \pm 0{\cdot}02$ at 25 cmH_2O (n.s.).

5. Capillary fenestrae ($8{\cdot}5 \pm 1{\cdot}1$ per fenestrated profile) and intercellular junctions were unaltered at high IAP. The tortuosity of the capillary-to-joint cavity path was $1{\cdot}50 \pm 0{\cdot}01$ below yield pressure and $1{\cdot}86 \pm 0{\cdot}24$ at 25 cmH_2O (n.s.).

6. Intra-articular tracers (ferrocyanide, ferritin and glycogen) permeated synovial interstitium without evidence of preferential pathways. Ferrocyanide delineated the capillary intercellular junction as a permeable channel. Ferritin and glycogen were phagocytosed by the macrophages.

7. In suprapatellar areolar synovium, the most extensive and most altered tissue, the ratio of interstitial area to path length increased maximally 4·1 times between 5 and 25 cmH_2O IAP. This represents a substantial contribution to the physiologically estimated rise in interstitial conductance (14 ×) but does not wholly explain it.

MS 7552

INTRODUCTION

The synovial lining of a diarthrodial joint is formed by fibroblast-like 'B cells' and macrophage-like 'A cells' (Graabeck, 1982; Mapp & Revell, 1987) but the cells are not linked by plasmalemmal junctions; they are separated by interstitium (Knight & Levick, 1984; Henderson & Pettipher, 1985). The latter allows fluid and solutes derived from the underlying capillaries to pass between the lining cells and form the intra-articular fluid, which lubricates the joint and nourishes the cartilage. Physiological studies of flow across the lining have established that the hydraulic conductance of the lining increases many times when intra-articular pressure (IAP) is raised above ~ 9 cmH_2O (yield point, Knight & Levick, 1985); such pressures occur naturally in joints containing effusions. In a search for a structural explanation, the synovial lining has been fixed *in situ* under a high IAP for microscopic examination. Scanning electron microscopy revealed stretching of the synovial surface at 25 cmH_2O IAP (McDonald & Levick, 1988). Light microscopy of histological sections showed a thinning of the lining, and the thickness of tissue separating the capillary network from the joint cavity was halved in the suprapatellar region (Levick & McDonald, 1989*a*). While this was a large effect it was nevertheless insufficient to explain fully the physiologically observed rise in conductance. The present study examines the effect of a high IAP on the ultrastructure of the transport pathways, using material from the same joints that were used in the histology study.

There is some controversy as to how fluid moves through interstitium and it has been suggested that specific matrix-deficient aqueous channels of width ~ 70 nm carry fluid through synovial interstitium (Casley-Smith & Vincent, 1978; Browning, 1980). This view is based partly on the uneven distribution of precipitated ferrocyanide, but the interpretation of the deposition pattern has been challenged (Aukland & Nicolaysen, 1981; Levick, 1983). The penetration of ferrocyanide from joint cavity into synovium was therefore also investigated.

In the Discussion the ultrastructural results on interstitial area are combined with the histological results on transport distance (Levick & McDonald, 1989*a*) to evaluate the interstitial area:distance ratio which, according to Darcy's law, governs the hydraulic conductance of a membrane for a given material permeability. The contribution of structural alterations to the synovial conductance change is thereby estimated.

METHODS

Synovial fixation under a controlled intra-articular pressure

Experiments were carried out on cannulated knees of New Zealand rabbits under anaesthesia (urethane, 500 mg kg^{-1} and pentobarbitone, 30 mg kg^{-1}). The procedures are described fully by Levick & McDonald (1989*a*), but in brief the trans-synovial flow of Krebs solution was measured at several IAPs during an initial hour of intra-articular infusion, then the synovium was fixed *in situ* at a known IAP by switching to an infusion reservoir containing buffered half-strength Karnovsky solution. Some tissue was fixed *in situ* at 5 cmH_2O IAP (below yield point, five joints). Control tissue was taken from five untreated joints and fixed by immersion. In five other joints synovium was fixed *in situ* at 25 cmH_2O IAP (above yield point). The initial flow measurements showed that the hydraulic conductance of the joint lining, expressed as change in trans-synovial

flow per unit change in IAP, had increased 4 times at 25 cmH_2O. This conductance is a composite of interstitial and endothelial conductances (Knight & Levick, 1985).

Electron-dense tracers

Ultrastructural tracer molecules were included in some intra-articular perfusates in an attempt to delineate any preferential interstitial pathways. Casley-Smith & Vincent (1978) suggested that ferrocyanide ions, which have a high negative charge density, might be excluded from negatively charged proteoglycan-rich areas and concentrate in any proteoglycan-deficient channels penetrating the interstitium. The location of ferrocyanide can be detected ultrastructurally after precipitation by acidic ferric acetate solution to form ferri–ferrocyanide complex (Prussian Blue). Browning (1980) developed a cobalt-based precipitant which preserves a more physiological pH and this method was used here. Sodium ferrocyanide (10 g l^{-1}) was added to the Krebs solution infused into one joint cavity at 5 cmH_2O IAP and one at 25 cmH_2O IAP. The NaCl concentration was reduced to 4·7 g l^{-1} to maintain osmolarity. The subsequent intra-articular fixative contained a cobalt salt, Tris(ethylenediamine) cobalt (III) chloride (10 g l^{-1}) at pH 7·4 prepared by the method of Work (1946). The cobalt salt diffuses into the tissue and forms an insoluble electron-dense complex on meeting ferrocyanide ions. For immersion-fixed samples the tissue was placed for 1 h in fixative containing ferrocyanide and then into a second fixative containing cobalt salt for 1 h. As further probes for distribution inhomogeneity, native horse spleen ferritin (radius, 5·5 nm; Sigma Chemical Co; 20 g l^{-1}) or rabbit liver glycogen (ultrastructural radius, 5 nm; Sigma; 50 g l^{-1}) were each infused into one joint at 5 cmH_2O IAP and one at 25 cmH_2O IAP. Ruthenium Red (Sigma Chemical Co, 1 g l^{-1}) was added to the fixative and buffer in six joints to stain interstitial polyanions such as proteoglycans and glycoproteins (Luft, 1971; Myers, 1976; Okada, Nakanishi & Kajikawa, 1981).

Sampling, sectioning and electron microscopy

Samples of suprapatellar areolar synovium, infrapatellar adipose synovium and posteromedial synovium were excised post-mortem, post-fixed in 1% osmium tetroxide and processed as described by Levick & McDonald (1989*a*); the same resin-embedded material was used in both studies. Preliminary sections were examined by light microscopy to check that sections were normal to the surface plane. Sections with a silver interference colour ($\sim$ 80 nm thick) were then cut with a glass knife on a Reichart–Jung ultramicrotome, collected on copper grids and stained with uranyl acetate in 30% ethanol (10 min) and lead citrate (8 min). Sections were examined in a Phillips 201 electron microscope at 80 kV. One section per block was photographed for morphometric analysis. At least 100 μm of the lining was photographed at low magnification (2000×) for morphometry of the intercellular space. Individual capillaries were photographed at medium magnification (4500–15000×), and fine features like fenestrae, endothelial junctions and interstitial fibrils were photographed at high magnification (70000×). The microscope magnification was calibrated with a 2160 lines mm^{-1} diffraction grating.

Measurements at low magnification (Fig. 1, upper frame)

Measurements were made by hand on micrographs printed at a further 2·5× magnification. Values are quoted without adjustment for macroscopic linear shrinkage, which averaged 7%. The following features were measured on low-magnification prints. (1) The length of synovial surface analysed (L). (2) Intercellular gap width, defined as distance between adjacent cytoplasmic profiles at the surface (G_0) and also in a parallel plane 5 μm beneath the surface (G_5). (3) The widths of each cytoplasmic profile at the surface, whether a cell body or merely a section of dendritic processes (C_w). (4) Any profile within 1 μm of the surface containing a nucleus was defined as a synovial lining cell body, and its width parallel to the surface plane (C_p) and normal to it (C_n) were measured. The ratio C_p/C_n served as an index of cell orientation. Cell bodies were categorized as either macrophage-like A cells (large vacuoles, Golgi bodies, filopodia) or fibroblast-like B cells (abundant rough endoplasmic reticulum) after Barland, Novikoff & Hamerman (1962) and Henderson & Pettipher (1985). (5) The interstitial volume fraction in all the tissue between the surface and a contour line 5 μm deep was estimated by the point-counting method, using a 24 × 16 cm square grid of 1 cm spaced points (384 points). The fraction of points lying over interstitium estimates the

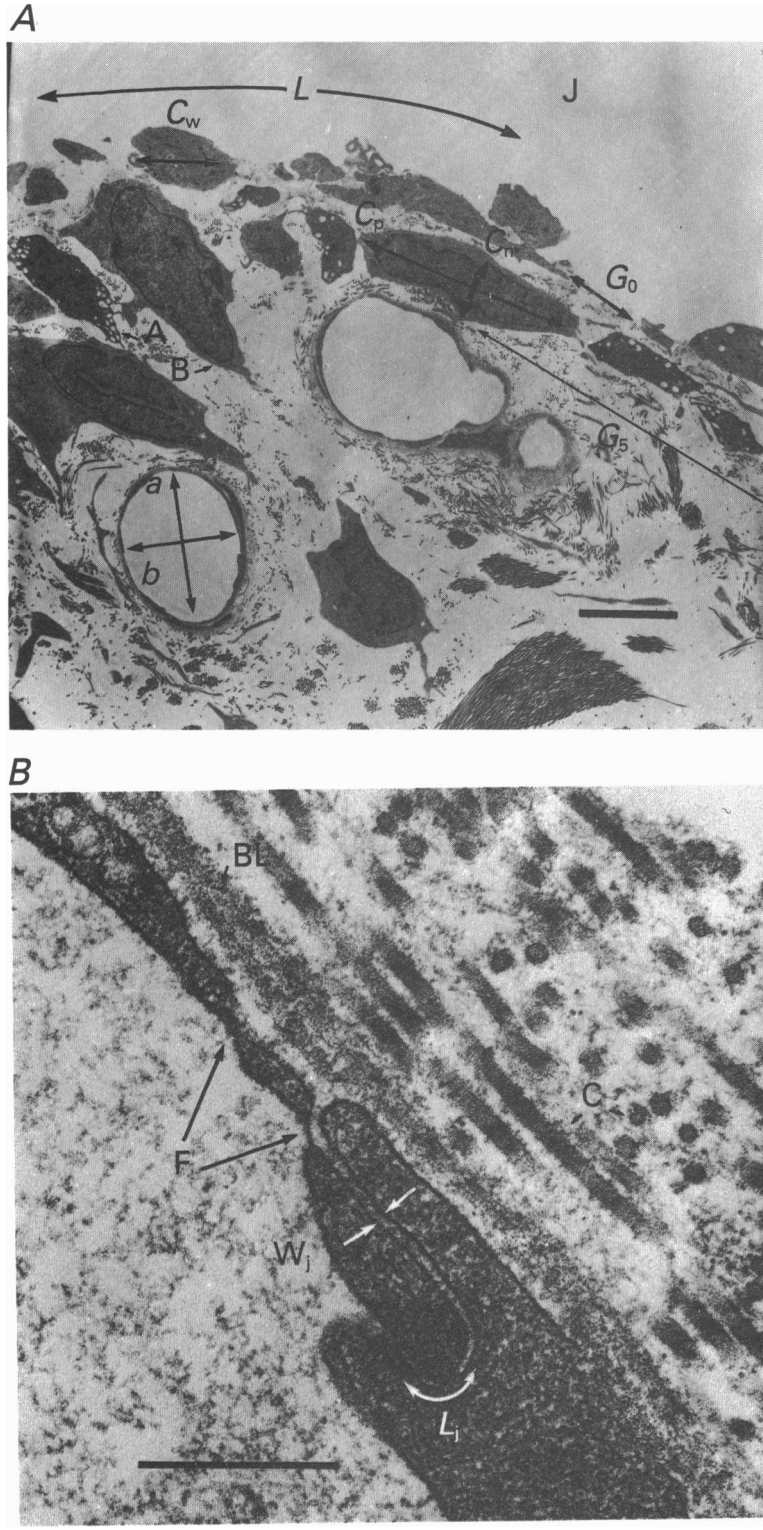

Fig. 1. For legend see facing page.

interstitial volume fraction (V_v). For each sample at least 800 points were counted to ensure a relative standard error of < 6% per measurement (Aherne & Dunhill, 1982).

Measurements at medium magnification

Capillaries were classified as fenestrated or continuous, and the major (a) and minor (b) internal axes were measured. The ratio a/b served as an index of capillary compression. Internal capillary circumference (C_c) was measured with a digitizer tablet linked to a Cambridge Electronics mini-computer. Small intraluminal endothelial flaps were ignored. The number of fenestrae per fenestrated capillary profile (N_f) and the presence or absence of fenestral diaphragms were recorded (Fig. 1*B*). Fenestral number density (D_f) was calculated as N_f/C_c.

Measurements at high magnification (see Fig. 1, lower frame)

Endothelial junction length (L_j) and width (W_j) were recorded. The latter was measured at the 'open' region. The number density of collagen fibrils in the collagen bundles (D_c) and the diameters of fibrils in transverse section were recorded.

Calculations and statistical analysis

The linear fraction of synovial surface occupied by interstitium was $\Sigma G_0/\Sigma L$. Since the line of cut for each sample fell randomly across the surface, Delesse's principle of equivalent linear and area fractions applies (Aherne & Dunnill, 1982) and $\Sigma G_0/\Sigma L$ is an estimate of the interstitial area fraction in the surface plane (A_{A_0}). Similarly the interstitial area fraction in the plane 5 μm below the surface (A_{A_5}) equals $\Sigma G_5/\Sigma L$.

The proportion of A and B cells was compared by the binomial test. Two populations were compared by the Mann–Whitney U test and multiple populations were compared by the multiple χ^2 test (Siegel, 1956) or by one-way analysis of variance with selected comparison by the conservative Scheffé test (Colquhoun, 1971). A probability of < 0·05 was accepted as significant. Means are followed by standard errors.

RESULTS

Forty-eight sections containing 6150 μm of synovial lining and 106 synovial capillaries were analysed. The principal findings were a marked stretching of the interstitial spaces at the synovial surface when IAP was raised to 25 cmH_2O (Fig. 2 and Table 1) and a change in synovial structure with distance from the surface.

Interstitial spaces at the surface

The lining cells' lack of junctions or basement membrane, reported by Ghadially & Roy (1966), was confirmed. The long cytoplasmic processes found extending over the surface in scanning electron micrographs (McDonald & Levick, 1988) were seen here as small non-nucleated surface profiles separated by a fibrous matrix. The interstitium-filled spaces ranged greatly in width, from 0·1 to 11·8 μm, and averaged ~ 2 μm (Table 1). The mean gap width was similar in immersion-fixed synovium and synovium fixed at 5 cmH_2O IAP. Raising IAP to 25 cmH_2O increased the mean gap

Fig. 1. Electron micrographs of synovium from rabbit knee illustrating morphometry. *A*, posteromedial synovium fixed *in situ* at low, endogenous intra-articular pressure. J, joint cavity. A, macrophage-like A cell. B, fibroblast-like B cell. Other symbols defined under 'Methods'. Control samples from other sites have a similar appearance. Scale bar = 5 μm. *B*, higher power showing a capillary intercellular junction and fenestrae (F), with diaphragms, one of which opens into the junction outlet. BL, basal lamina. C, periodic collagen fibril. For other symbols see 'Methods', Scale bar = 400 nm.

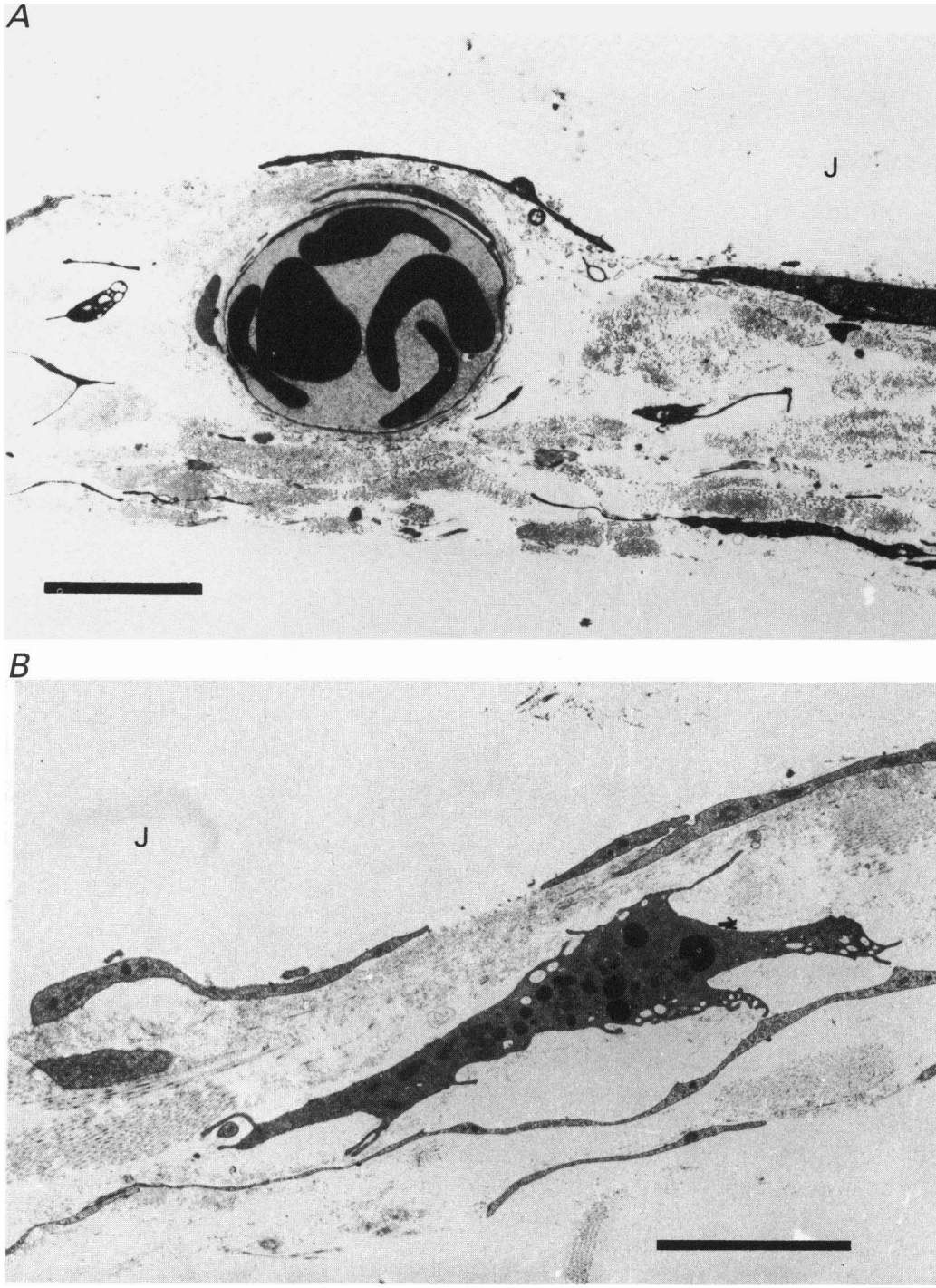

Fig. 2. Two examples of synovium from suprapatellar pouch fixed *in situ* at an intra-articular pressure of 25 cmH_2O. J, joint cavity. In *A* note slight bulge into joint cavity caused by well-filled microvessel. *B* contains an A cell. Scale bars = 5 μm.

width to 3·1 μm in both areolar and adipose synovium ($P < 0.01$ and $P < 0.05$ respectively by Scheffé's test). Posteromedial synovium showed no significant change, for which there was no obvious explanation. Interstitium formed 26–35% of the synovial surface at low IAP and 23–45% at 25 cmH_2O IAP (differences not significant).

TABLE 1. Morphometry of interstitial spaces in the synovial lining of the rabbit knee (mean ± S.E.M., n)

		Fixation condition		
			IAP	
Tissue sample	Measurement*	Immersion	5 cmH_2O	25 cmH_2O
Areolar	G_0 (μm)	1·97 ± 0·18 (121)	2·19 ± 0·26 (79)	3·11 ± 0·34 (89)
	G_5 (μm)	4·11 ± 0·35 (127)	7·04 ± 0·81 (54)	6·87 ± 0·89 (54)
	A_{A_0}	0·33 ± 0·07 (5)	0·35 ± 0·06 (5)	0·45 ± 0·03 (5)
	A_{A_5}	0·67 ± 0·04 (5)	0·58 ± 0·05 (5)	0·61 ± 0·04 (5)
Adipose	G_0 (μm)	1·94 ± 0·26 (91)	1·88 ± 0·19 (103)	3·09 ± 0·39 (74)
	G_5 (μm)	4·57 ± 0·56 (62)	7·57 ± 1·26 (58)	9·67 ± 1·35 (42)
	A_{A_0}	0·28 ± 0·08 (5)	0·31 ± 0·05 (5)	0·35 ± 0·07 (5)
	A_{A_5}	0·44 ± 0·08 (5)	0·69 ± 0·02 (5)	0·62 ± 0·05 (5)
Posteromedial	G_0 (μm)	2·09 ± 0·21 (73)	2·38 ± 0·24 (79)	1·77 ± 0·19 (80)
	G_5 (μm)	4·91 ± 0·78 (66)	5·41 ± 0·69 (69)	6·27 ± 1·00 (51)
	A_{A_0}	0·26 ± 0·06 (5)	0·29 ± 0·05 (5)	0·23 ± 0·05 (5)
	A_{A_5}	0·50 ± 0·06 (5)	0·55 ± 0·07 (5)	0·49 ± 0·11 (5)

* G denotes width of interstitial gap in a plane parallel to surface, either along the surface (G_0) or 5 μm deep to the surface (G_5). A_A is the interstitial area fraction ($= \Sigma G/L$) forming surface (A_{A_0}) or 5 μm beneath it (A_{A_5}).

Interstitial spaces 5 μm below the surface

The 5 μm plane was selected for morphometry because it represents roughly the lower end of the extravascular component of the blood–joint barrier, judging by the harmonic mean capillary depth (Levick & McDonald, 1989*a*). The spaces between the cytoplasmic profiles were typically about twice as wide at 5 μm depth (G_5) as at the surface (G_0) in all three kinds of synovium ($P < 0.001$, U test). The interstitial area fraction too increased with depth and formed up to 69% of the plane 5 μm below the surface (Fig. 3; $P < 0.002$ under all conditions, U test). Elevation of IAP from 5 to 25 cmH_2O did not significantly alter the interstitial gap width or fractional area at the 5 μm contour. There was, however, a consistent difference between gap width in immersion-fixed tissue and tissue fixed *in situ* at 5 cmH_2O ($P < 0.05$, analysis of variance), perhaps due to the retraction of unfixed tissue during excision.

The fraction of the tissue between the surface and the 5 μm contour which consisted of interstitium (V_V) was 0·54 ± 0·05 after immersion-fixation, 0·61 ± 0·05 at 5 cmH_2O IAP and 0·67 ± 0·02 at 25 cmH_2O in areolar synovium. These differences were not significant on analysis of variance.

As well as quantitative changes with depth, there were distinct qualitative changes in fibrillar composition. At depths greater than 2–5 μm, bundles of coarse periodic collagen fibrils abounded, of diameter 55 ± 3 nm in areolar and posteromedial synovium (twenty-nine bundles) or 43 ± 3 nm in adipose synovium (thirteen bundles;

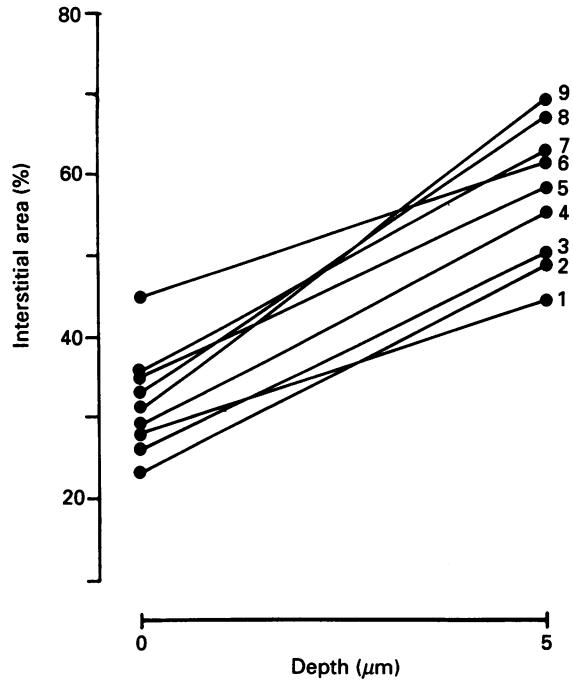

Fig. 3. Change in tissue composition with distance normal to the synovial surface. Line numbers identify sample site and fixation method. Suprapatellar areolar synovium is lines 8 (immersion fixed), 5 (5 cmH_2O IAP) and 6 (25 cmH_2O IAP); infrapatellar adipose synovium, lines 1 (immersion), 9 (5 cmH_2O IAP) and 7 (25 cmH_2O IAP); posteromedial synovium, lines 3 (immersion), 4 (5 cmH_2O IAP) and 2 (25 cmH_2O IAP). Standard error bars omitted for clarity.

$P < 0{\cdot}01$). Immunohistochemistry of the lining using monoclonal antibodies confirmed the presence of type I and type III collagens, the collagens of classic periodic fibrils, and also the presence of type V collagen (D. E. Ashhurst & J. R. Levick, unpublished observations). At the surface by contrast there were only isolated scattered periodic fibrils, of smaller diameter (32 ± 2 nm; $P < 0{\cdot}01$) but there was an abundant irregular meshwork of fine microfibrils of mean diameter $9{\cdot}3 \pm 0{\cdot}7$ nm ($n = 15$). The microfibrils stained densely with Ruthenium Red and were associated with broader striped bundles called fibrous long-spacing bundles (period $92{\cdot}8 \pm 2{\cdot}8$ nm). Their possible relation to type VI collagen is discussed by Levick & McDonald (1989*b*). Elevation of IAP to 25 cmH_2O caused the microfibrillar meshwork to become increasingly oriented in the plane of the surface, indicating an increased surface stress.

The synovial lining cells (see Table 2)

Out of 219 nucleated profiles a third were identified as macrophage-like A cells, the rest as B cells, confirming the predominance of the latter in young rabbit synovium (Krey & Cohen, 1973; Jilani & Ghadially, 1986). The ratio of cells was not

TABLE 2. Morphometry of synovial lining cells* (nucleated profiles; mean ± S.E.M., *n*)

		Fixation condition		
			IAP	
Tissue sample	Measurement†	Immersion	5 cmH_2O	25 cmH_2O
Areolar	A cells (%)	33	33	56
	C_p (μm)	9·22 ± 0·79 (27)	15·74 ± 2·00 (14)	13·08 ± 1·48 (18)
	C_n (μm)	3·90 ± 0·34 (27)	2·81 ± 0·27 (14)	2·28 ± 0·44 (18)
	C_p/C_n	2·67 ± 0·28 (27)	6·56 ± 1·15 (14)	8·29 ± 1·87 (18)
Adipose	A cells (%)	37	26	24
	C_p (μm)	11·06 ± 0·73 (28)	10·83 ± 1·32 (18)	12·15 ± 1·60 (16)
	C_n (μm)	4·23 ± 0·41 (28)	3·05 ± 0·25 (18)	3·49 ± 0·32 (16)
	C_p/C_n	3·42 ± 0·40 (28)	4·37 ± 0·78 (18)	3·94 ± 0·09 (16)
Posterior	A cells (%)	24	30	30
	C_p (μm)	13·67 ± 1·68 (22)	13·71 ± 1·80 (18)	14·17 ± 1·14 (18)
	C_n (μm)	5·09 ± 0·48 (22)	4·42 ± 0·45 (18)	2·65 ± 0·28 (18)
	C_p/C_n	3·81 ± 0·65 (22)	3·81 ± 0·61 (18)	5·86 ± 0·53 (18)

* Defined as nucleated profiles with the superficial pole no deeper than 1 μm beneath the synovial surface.

† C_p = maximum cell width in plane parallel to surface; C_n = maximum cell length in direction normal to surface.

significantly altered on raising IAP (χ^2 test). The cell dimensions (8–16 μm wide by 3–7 μm deep) were similar to human synoviocytes (8–12 μm × 6–8 μm; Castor, 1960), with the long axis of the cell in general parallel to the surface. The orientation index C_p/C_n (Table 2) was greater at 25 cmH_2O IAP, in keeping with the impression of cell elongation (e.g. Fig. 2; also McDonald & Levick, 1988) but only the differences between immersion-fixed synovium and synovium at 25 cmH_2O reached statistical significance ($P < 0·05$, analysis of variance). The width of the cytoplasmic profiles at the surface (C_w, see Methods) averaged 3·84 ± 0·32 μm ($n = 121$, areolar synovium) to 5·86 ± 0·68 μm ($n = 88$, posteromedial synovium), and was not significantly changed at high IAP.

Capillary size and compression

The reduction in capillary size after immersion fixation, and the absence of statistically significant change in size or compression (axial ratio) between 5 and 25 cmH_2O IAP (Table 3) mirror the findings in our histological studies (Levick & McDonald, 1989*a*) and are discussed there. The increased proximity of the capillaries to the surface at the higher IAP described by Levick & McDonald (1989*a*) is evident on comparing Figs 1 and 2 here, and it is clear from Fig. 2 that capillaries remained patent despite an extremely superficial location at 25 cmH_2O IAP.

Capillary wall pathways: fenestrations, junctions and vesicles (see Figs 1 and 4)

Roughly half of the capillary profiles (50/106) contained fenestrae, which are thin windows of high hydraulic conductance. Although adipose synovium contained a greater proportion of fenestrated profiles (63%) than areolar synovium (39%), as

TABLE 3. Morphometry of synovial lining capillaries (mean ± S.E.M., n)

		Fixation condition		
			IAP	
Tissue	Measurement*	Immersion	5 cmH_2O	25 cmH_2O
Areolar	C_c (μm)	18·0 ± 3·1 (21)	32·1 ± 9·3 (8)	27·3 ± 3·8 (12)
	a/b	2·64 ± 0·56 (21)	2·22 ± 0·56 (8)	1·87 ± 0·31 (12)
	Fenestrated capillaries	6/21	3/8	8/12
	D_f (μm^{-1})	0·48 ± 0·15 (6)	0·26 ± 0·13 (3)	0·30 ± 0·11 (8)
	D_{icj} (μm^{-1})	0·17 ± 0·02 (21)	0·09 ± 0·01 (8)	0·09 ± 0·01 (11)
Adipose	C_c (μm)	15·3 ± 2·0 (12)	18·9 ± 3·4 (10)	22·0 ± 3·1 (10)
	a/b	2·31 ± 0·28 (12)	2·53 ± 0·37 (10)	2·46 ± 0·48 (10)
	Fenestrated capillaries	8/12	4/10	8/10
	D_f (μm^{-1})	0·49 ± 0·14 (8)	0·47 ± 0·08 (4)	0·37 ± 0·08 (8)
	D_{icj} (μm^{-1})	0·17 ± 0·04 (12)	0·09 ± 0·02 (10)	0·08 ± 0·02 (10)
Posterior	C_c (μm)	18·0 ± 2·4 (11)	23·3 ± 4·1 (8)	17·7 ± 1·1 (13)
	a/b	2·33 ± 0·42 (11)	2·89 ± 0·55 (8)	2·07 ± 0·34 (13)
	Fenestrated capillaries	6/12	2/8	4/13
	D_f (μm^{-1})	0·58 ± 0·32 (6)	0·29— (2)	0·44 ± 0·16 (4)
	D_{icj} (μm^{-1})	0·12 ± 0·03 (11)	0·12 ± 0·03 (7)	0·10 ± 0·01 (13)

* C_c is the circumference of the capillary profile and a/b is the ratio of its major to minor axes. 'Fenestrated capillaries' represents the number of profiles bearing fenestrae out of total profiles observed, and D_f is the number of fenestrae per micrometre circumference. D_{icj} is the number of intercellular junctions per micrometre circumference.

originally reported by Suter & Majno (1964), the difference was not statistically significant. A densely staining diaphragm ~ 4 nm thick spanned 425 out of 426 fenestrae; but there is physiological evidence that the diaphragm contributes little to the hydraulic resistance of the fenestral pathway (Levick & Smaje, 1987). The fenestral density (8·5 ± 1·1 per fenestrated profile) was not significantly influenced by IAP or tissue type (Table 3). Similarly, the number of endothelial cell junctions per profile (1·9 ± 0·1, $n = 103$), their lengths (730 ± 70 nm) and widths (18·7 ± 1·2 nm) were unaltered by raising IAP. There was no evidence of inflammation in the form of junction separation or polymorph adhesion in 105/106 capillaries, so the yield phenomenon is unlikely to be caused by inflammation, as indeed the high albumin reflection coefficient also indicates (Levick & Knight, 1988). In just one intimal capillary an adherent marginating polymorph was found after ferritin infusion. The endothelial vesicles were not analysed morphometrically but there was no obvious change in their size or density on inspection. Fused multivesicular transendothelial channels were not seen. The capillary basement membrane appeared unaltered at high IAP.

Tortuosity of the joint-to-capillary pathway

The least distance which fluid has to traverse between the joint cavity and pericapillary space was assessed in our histological study by straight line measurements (Levick & McDonald, 1989*a*). The electron micrographs show however, that the true pathway involves a tortuous route imposed by the irregular synovial lining cells (Fig. 1). Tortuosity was quantified as the shortest distance which could be traced from the joint cavity to the nearest point on a synovial capillary without crossing a cell membrane, divided by the length of a straight line between the starting and finishing points. Overall the tortuosity factor averaged $1{\cdot}50 \pm 0{\cdot}10$ for fifty-three interstitial routes. A slight increase in the tortuosity factor at 25 cmH_2O IAP ($1{\cdot}86 \pm 0{\cdot}24$, $n = 18$) was not statistically significant relative to tortuosity at 5 cmH_2O IAP ($1{\cdot}45 \pm 0{\cdot}28$, $n = 7$) or immersion-fixed synovium ($1{\cdot}45 \pm 0{\cdot}10$, $n = 24$; analysis of variance).

Distribution of electron-dense particles

The distribution of ferritin and glycogen in the interstitium appeared random, and both were taken up into the vesicles of A cells. The distribution of ferrocyanide precipitate proved most interesting in view of its previous usage to delineate 'preferential flow channels'.

Deposits of Tris(ethylenediamine) cobalt (III) ferrocyanide occurred throughout the interstitial matrix in the form of needles $\sim$ 10–30 nm wide $\times$ 100–350 nm long and as clumps of diameter 100–300 nm. More homogeneous curved bands of deposit formed within some collagen bundles, suggestive of a diffusion front. None of these corresponded to the 70 nm diameter ovoids observed by Casley-Smith & Vincent (1978) with acidic ferric acetate as precipitant. Capillary deposits were interesting in two respects. First, a dense precipitate filled the endothelial cell cleft (Fig. 4*A*), an observation analogous to early ion-precipitation evidence that the endothelial cleft forms a transcapillary pathway for small solutes and by implication water (e.g. Casley-Smith, 1967). Second, clumps of deposit did not occur solely in the interstitium; identical clumps were found in the capillary lumen too (Fig. 4*B*), and this seems to cast serious doubt on the view that localized ferrocyanide deposits reflect local inhomogeneities in the distribution of negatively charged proteoglycans (Casley-Smith & Vincent, 1978). The interstitial ferrocyanide deposits could not be interpreted as evidence for preferential flow channels in our study. It is also relevant to note that the endothelial cleft was well labelled despite the known existence of fixed negative charges in the endothelial glycocalyx.

DISCUSSION

Interstitial structure below yield pressure

Bare interstitium formed a substantial proportion of the cavity lining in this study (26–33%), as in earlier work (Knight & Levick, 1984, 17–21%; McDonald & Levick, 1988, 18–29%). It is unlikely that the interstitial exposure was a dehydration artifact since the specimen shrinkage was only 7% and since interstitial exposure was first described in fully hydrated specimens, in a little-known paper by Braun

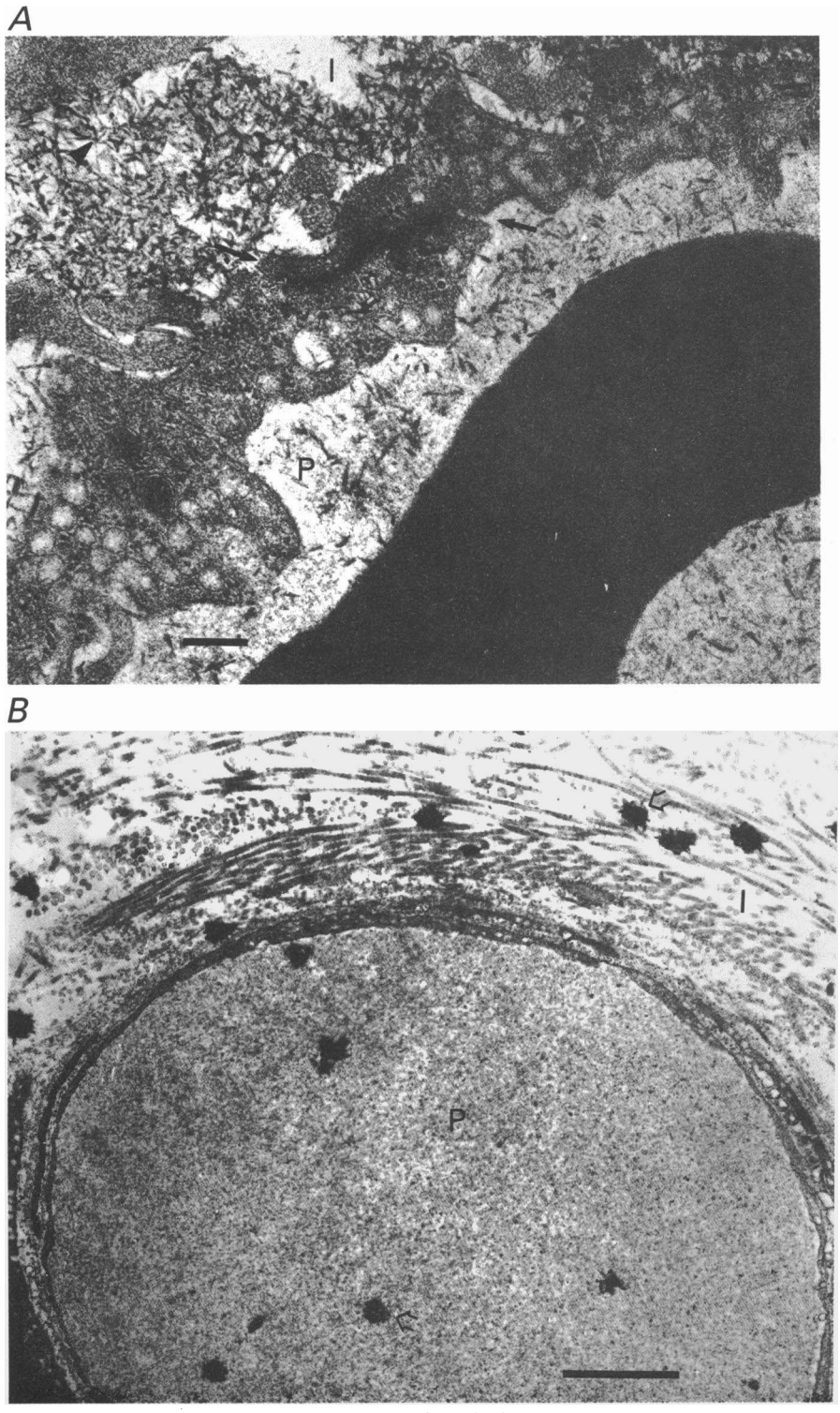

Fig. 4. For legend see facing page.

(1894). A spacious pathway is thus available for fluid exchange across the synovial surface. The finding that the interstitial pathway grows broader still at greater depth appears to be new. The difference is probably the result of the tendency of the cells to spread cytoplasmic processes over the surface but not below it (McDonald & Levick, 1988), and it introduces some difficulties into the interpretation of conductance changes (see later). The change in structure normal to the surface proved to be qualitative as well as quantitative since the innermost interstitium has a fine microfibrillar network and a paucity of periodic collagen fibrils. Both ferritin and glycogen (radius 5–5·5 nm) were able to penetrate the microfibrillar meshwork and other elements and this is consistent with an estimate of 10–15 nm for the mean hydraulic radius of synovial interstitium, based on interpolation of data in Levick (1987). Tracer distribution gave no hint of preferential channels within the interstitium, and the ferrocyanide distribution leads us to doubt the value of this approach as a probe for preferential flow channels.

Synovial capillary structure; lack of effect of IAP

The observation that a high IAP produced no inflammation and no structural alteration in the generally accepted fluid pathways across the capillary wall (fenestrae and clefts) is consistent with the view, based on physiological evidence, that the yield phenomenon does not originate in the capillary wall. The absence of collapse of the lining capillaries at 25 cmH_2O IAP was discussed by Levick & McDonald (1989*a*).

Deformation of the interstitial pathway at 25 cmH_2O

A high IAP produced a marked widening of the interstitial spaces at the synovial surface, especially in areolar synovium, and possibly a modest (28%; n.s.) increase in pathway tortuosity due to cell elongation. The increase in gap width and hence interstitial area was presumably caused by a tangential stress set up by the distending pressure (Laplace's law), which would also explain the increased alignment of the superficial microfibrillar network at 25 cmH_2O. As well as the increase in absolute interstitial area there may have been a modest increase in interstitial area fraction at the surface: this change did not achieve statistical significance here but a similar increase in fractional area was observed by scanning electron microscopy in other joint samples (McDonald & Levick, 1988). An increase in the fractional area would imply that the superficial interstitium expanded more than the cellular elements, which could be due to increased interstitial hydration or to incorporation of interstitium from a slightly deeper plane where the interstitial area fraction is greater (Fig. 3).

Fig. 4. Pattern of deposition of cobalt–ferrocyanide complex after counterstaining. *A* shows needle-shaped deposits in interstitium (arrow-head) and in plasma at a lower concentration, in immersion-fixed synovium. Arrows mark an endothelial intercellular cleft filled with ferrocyanide deposit. I, interstitium; P, plasma. scale bar = 200 nm. *B* shows clumping of deposits into larger aggregates in synovium fixed *in situ* at 25 cmH_2O IAP. Note presence of clumps in plasma of a fenestrated capillary as well as in interstitium (arrows). Scale bar = 1 μm.

A histological study of the same tissue showed that the synovial lining and the blood-to-joint component became thinner at 25 cmH_2O IAP, especially in the suprapatellar areolar–muscular synovium (Levick & McDonald, 1989*a*). The combined picture from the histological and ultrastructural studies is therefore one of a reduction in the path length for fluid exchange (even allowing for an increase in tortuosity) and an increase in area available for exchange at the surface, particularly in the suprapatellar pouch, which is the largest compartment of the knee. An increase in area (A) and a decrease in path length (Δx) will increase interstitial conductance, according to Darcy's law of flow.

Change in $A/\Delta x$ compared with change in conductance

While the observed geometrical changes must enhance conductance, they may not be sufficient in themselves to explain fully the large conductance changes. For the net plasma-to-joint pathway (endothelium plus interstitium) the conductance increases 4·9 times between 4–6 and 25 cmH_2O IAP (Knight & Levick, 1985). Since the conductance of the capillary wall is constant and is arranged in series with the interstitial path, the interstitial conductance must increase much more than 4·9 times to explain the rise in net barrier conductance; an increase in interstitial conductance by 14·2 times is required. We will therefore assess whether the maximum observed geometric change could produce such a conductance increase. In suprapatellar synovium, the most deformed and extensive tissue, the width of the surface gaps increased by a factor 3·11/2·19, i.e. 1·42 times between 5 cmH_2O and 25 cmH_2O. The increase in interstitial area is proportional to the square of the linear increase, giving a factor of 2·02. The harmonic mean depths of capillary near-edges fell from 3·7 to 1·82 μm, a factor of 0·49. Thus the maximum increase in the Darcy geometric term $A/\Delta x$ was 2·02/0·49 or 4·12 times for the supracapillary interstitial path. This may be partially offset by a 1·28 times increase in path tortuosity, giving a maximum increase in $A/\Delta x$ of 3·22 times. This result is an upper limit since (a) it is based on areolar synovium, where changes were most pronounced; (b) interstitial area changed relatively more at the surface than 5 μm beneath it; and (c) the shift in capillary centre is proportionately smaller than the shift in capillary near-edge. It seems clear from this simple calculation that although the observed interstitial deformation can contribute substantially to the conductance increase, the latter is by no means fully explained. A similar conclusion is reached on comparing the change in the conductance of the full thickness of synovium (circulatory arrest results of Levick, 1980) with the change in synovial lining thickness and area, though the discrepancy is less marked here.

The hydration of a stressed deformable matrix

In general terms conductance depends on $A/\Delta x$ and on the specific hydraulic conductivity of the material (K), and in the case of fibrous materials like interstitium K is very sensitive to fibre concentration and thus hydration (e.g. Bert & Fatt, 1970; Levick, 1987). Fisher (1982) studied conductance changes in isolated lens capsule basement membrane and observed that $A/\Delta x$ increased on raising the transmural pressure but did not explain the change in conductance, which actually declines in this tissue. The membrane's void volume (hydration) declined too. This leads us to

consider the interaction of hydraulics and mechanics in a stressed deformable membrane – a complex matter owing to opposing trends. In an aorta pressurized with air for example, the mechanical stresses *per se* tend to compact the interstitium and reduce hydration; but if the aorta is pressurized with water, the concomittant hydraulic flow through the tissue partially prevents compaction, and in de-endothelialized aorta will even increase the hydration (Tedgui & Lever, 1987).

In synovium, $A/\Delta x$ increased 3·22–4·12 times at most, so K would have to increase at least 4·41–3·45 times to create a 14·2-fold rise in interstitial conductance ($KxA/\Delta x$). Interpolating from the logarithmic plots of hydration against K in the above references, we find that a 3·4- to 4·4-fold rise in K would require either that interstitial volume increases 1·9–2·4 times for a fixed fibre content, or that 42%–54% of the fibre content is lost at constant tissue volume, or some intermediate combination of fluid gain and fibre loss.

The morphometric evidence relating to synovial hydrational changes unfortunately did not give a clear-cut result. The surface interstitial area fraction A_A and the interstitial volume fraction V_v both increased between 5 and 25 cmH_2O IAP – but without statistical significance and by only 29 and 10% respectively. The number density of capillaries failed to decrease (Levick & McDonald, 1989*a*), the number density of collagen fibrils within a bundle (147 ± 10 to $165 \pm 20\ \mu m^{-2}$) did not decrease, and collagen fibril diameter, which in cartilage displays a modest dynamic sensitivity to proteoglycan concentration (Maroudas & Bannon, 1981) was constant. It seems unlikely from these results that interstitial volume could have doubled (see previous paragraph). This focuses attention on the other potential factor noted above, a wash-out of poorly anchored molecular fibres (glycosaminoglycans) from the superficial microfibrillar network, which might preferentially increase supra-capillary interstitial conductivity. Histochemical and biochemical studies will be needed to address these issues.

This study was funded by the Arthritis and Rheumatism Council of Great Britain.

REFERENCES

AHERNE, W. A. & DUNHILL, M. S. (1982). *Morphometry*. Edward Arnold, London.

AUKLAND, K. & NICOLAYSEN, G. (1981). Interstitial fluid volume: local regulatory mechanisms. *Physiological Reviews* **61**, 560–561.

BARLAND, P. A., NOVIKOFF, A. B. & HAMERMAN, K. D. (1962). Electron microscopy of the human synovial membrane. *Journal of Cell Biology* **14**, 207–220.

BERT, J. L. & FATT, I. (1970). Relation of water transport to water content in swelling biological membranes. In *Surface Chemistry of Biological Systems*, ed. BLANK, M. pp. 287–294. New York, Plenum Press.

BRAUN, H. (1984). Untersuchungen über den Bau der Synovialmembranen und Gelenkknorpel, sowie über die Resorption flüssiger und fester Körper aus den Gelenkhölen. *Deutsche Zeitschrift für Chirurgie* **39**, 35–86.

BROWNING, J. (1980). Demarcation of tissue channels by ferrocyanide deposits: use of an alternative precipitant. *Microvascular Research* **19**, 380–384.

CASLEY-SMITH, J. R. (1967). An electron microscope study of the passage of ions through the endothelium of lymphatics and blood capillaries and through the mesothelium. *Quarterly Journal of Experimental Physiology* **52**, 105–113.

CASLEY-SMITH, J. R. & VINCENT, A. H. (1978). The quantitative morphology of interstitial tissue channels in some tissues of the rat and rabbit. *Tissue and Cell* **10**, 571–584.

CASTOR, C. W. (1960). The microscopic study of normal human synovial tissue. *Arthritis and Rheumatism* **3**, 140–151.

COLQUHOUN, D. (1971). *Lectures on Biostatistics*, pp. 171–213. Oxford, Clarendon Press.

FISHER, R. F. (1982). The water permeability of basement membrane under increasing pressure: evidence for a new theory of permeability. *Proceedings of the Royal Society* B **216**, 475–496.

GHADIALLY, F. N. & ROY, S. (1966). Ultrastructure of rabbit synovial membrane. *Annals of the Rheumatic Diseases* **25**, 318–326.

GRAABAEK, P. M. (1982). Ultrastructural evidence for two distinct types of synoviocytes in rat synovial membrane. *Journal of Ultrastructural Research* **78**, 321–339.

HENDERSON, B. & PETTIPHER, E. R. (1985). The synovial lining cell: biology and pathobiology. *Seminars in Arthritis and Rheumatism* **15**, 1–32.

JILANI, M. & GHADIALLY, F. N. (1986). An ultrastructural study of age-associated changes in the rabbit synovial membrane. *Journal of Anatomy* **146**, 201–215.

KNIGHT, A. D. & LEVICK, J. R. (1984). Morphometry of the ultrastructure of the blood–joint barrier in the rabbit knee. *Quarterly Journal of Experimental Physiology* **69**, 217–288.

KNIGHT, A. D. & LEVICK, J. R. (1985). Effects of fluid pressure on the hydraulic conductance of interstitium and fenestrated endothelium in the rabbit knee. *Journal of Physiology* **360**, 311–332.

KREY, P. R. & COHEN, A. S. (1973). Fine structural analysis of rabbit synovial cells. I. The normal synovium and changes in organ cultures. *Arthritis and Rheumatism* **16**, 324–340.

LEVICK, J. R. (1980). Contributions of the lymphatic and microvascular systems to fluid absorption from the synovial cavity of the rabbit knee. *Journal of Physiology* **306**, 445–461.

LEVICK, J. R. (1983). Synovial fluid dynamics: the regulation of volume and pressure. In *Studies in Joint Disease 2*, ed. MAROUDAS, A. & HOLBOROW, E. J., pp. 166–167. Pitman, London.

LEVICK, J. R. (1987). Flow through interstitium and other fibrous matrices. *Quarterly Journal of Experimental Physiology* **72**, 409–43.

LEVICK, J. R. & KNIGHT A. D. (1988). Interaction of plasma colloid osmotic pressure and joint fluid pressure across the endothelium–synovium layer: significance of extravascular resistance. *Microvascular Research* **35**, 109–121.

LEVICK, J. R. & SMAJE, L. H. (1987). An analysis of the permeability of a fenestra. *Microvascular Research* **33**, 233–256.

LEVICK, J. R. & McDONALD, J. N. (1989*a*). Synovial capillary distribution in relation to altered pressure and permeability in knees of anaesthetized rabbits. *Journal of Physiology* **419**, 477–492.

LEVICK, J. R. & McDONALD, J. N. (1989*b*). The microfibrillar meshwork of the synovial lining and associated broad-banded collagen – a clue to identity. *Annals of the Rheumatic Diseases* (in the Press).

LUFT, J. H. (1971). Ruthenium Red and Violet. II. Fine structural localization in animal tissues. *Anatomical Record* **171**, 369–415.

McDONALD, J. N. & LEVICK, J. R. (1988). Morphology of surface synoviocytes in situ at normal and raised joint pressure, studied by scanning electron microscopy. *Annals of the Rheumatic Diseases* **47**, 232–240.

MAPP, P. I. & REVELL, P. A. (1987). Ultrastructural localisation of muramidase in the human synovial membrane. *Annals of the Rheumatic Diseases* **46**, 30–37.

MAROUDAS, A. & BANNON, C. (1981). Measurement of swelling pressure in cartilage and comparison with the osmotic pressure of constituent proteoglycans. *Biorheology* **18**, 619–632.

MYERS, D. B. (1976). Electron microscopic autoradiography of $^{35}SO_4$-labelled material closely associated with collagen fibrils in mammalian synovium and ear cartilage. *Histochemical Journal* **8**, 191–199.

OKADA, Y., NAKANISHI, I. & KAJIKAWA, K. (1981). Ultrastructure of the mouse synovial membrane. Development and organization of the extracellular matrix. *Arthritis and Rheumatism* **24**, 835–843.

SIEGEL, S. (1956). *Nonparametric Statistics for the Behavioural Sciences*. McGraw-Hill Kogakusha Ltd, Tokyo.

SUTER, E. R. & MAJNO, G. (1964). Ultrastructure of the joint capsule in the rat: presence of two kinds of capillaries. *Nature* **202**, 920.

TEDGUI, A. & LEVER, M. J. (1987). Effect of pressure and intimal damage on ^{131}I-albumin and [^{14}C]sucrose spaces in aorta. *American Journal of Physiology* **235**, H1530–1539.

WORK, J. B. (1946). Tris(ethylenediamine) cobalt(III) chloride. *Inorganic Synthesis* **2**, 221–222.